*Article*

# A Comparative Analysis of Vanadyl Porphyrins Isolated from Resins of Heavy Oils with High and Low Vanadium Content

Makhmut Yakubov [ID], Guzalia Abilova [ID], Elvira Tazeeva, Svetlana Yakubova *[ID], Damir Tazeev, Nikolay Mironov [ID] and Dmitriy Milordov

FRC Kazan Scientific Center, Arbuzov Institute of Organic and Physical Chemistry, Russian Academy of Sciences, 420088 Kazan, Russia; yakubovmr@mail.ru (M.Y.); abiliti7@yandex.ru (G.A.); tazeeva_elvira@mail.ru (E.T.); tazeevexc4@yahoo.com (D.T.); n_mir@mail.ru (N.M.); milordoff@yandex.ru (D.M.)
* Correspondence: yakubovasg@mail.ru; Tel.: +7-(843)-272-73-44

**Abstract:** The composition of purified vanadyl porphyrins recovered from the resins of heavy oils possessing high and low vanadium contents was investigated. Vanadium content in the resins of the heavy oils under study differs by a factor of ca. 15. To recover and purify vanadyl porphyrins from the resins, extraction by *N,N*–dimethylformamide (DMF) with subsequent two-stage column chromatography on silica gel and sulfocationite were employed. The change of structural-group composition and content of vanadyl porphyrins in the products obtained at each stage was evaluated using Fourier IR and UV-Vis spectroscopy. Analysis of the purified vanadyl porphyrins using MALDI mass spectrometry determined distribution of their most abundant types (etio- and DPEP) and identified $C_{27}$–$C_{39}$ homologs for the resins possessing high vanadium content and $C_{28}$–$C_{39}$ homologs for the resins with low vanadium content.

**Keywords:** heavy oil; resins; vanadium; vanadyl porphyrins; extraction; chromatography; spectroscopy; MALDI mass spectrometry

## 1. Introduction

Growing demand in motor fuels stimulates an increase in recovery and upgrading of heavy oil (HO) featuring a high content of resinous and asphaltene components and heteroatomic sulfur-, nitrogen-, and oxygen-containing compounds, as well as vanadyl and nickel metal complexes [1,2]. The main schemes of heavy oil upgrading are based on the removal of excess carbon (carbonization, cracking, and deasphaltization) or introduction of additional hydrogen (hydrorefining). The choice of hydrorefining technologies of heavy hydrocarbon crude primarily depends on the metal content, mainly V and Ni. In the metal concentration range of 10–100 ppm, fixed-bed catalytic hydrocracking is preferable. Fluidized-bed catalytic cracking with recycling and periodic replacement of catalyst is used at the concentrations of metals of >100 ppm. Heavy oil with the metal content of $\geq$1000 ppm can be upgraded by slurry processes using nanosized catalysts [3–6]. Vanadium and nickel are mainly represented by metalloporphyrins in oils, which can form associates with asphaltenes [7,8].

Petroleum metalloporphyrins are related to geochemical biomarkers and provide information on the maturation of oils and source beds; they are also applicable for evaluation of thermal maturity of deposits and oils [9,10]. Petroleum metalloporphyrins are mainly represented by following homologous series: etio-, deoxophylloerythroetio- (DPEP), dicyclodeoxophylloerythroetio-(di-DPEP) porphyrins, as well as their rhodo-derivatives (rhodo-etio, rhodo-DPEP, and Rhodo-Di-DPEP) [11]. The ratio of relative abundance of vanadyl porphyrins of DPEP type to those of etio type is an important criterion for the study of source of oil and its maturity. Chlorophyll acts as a source of DPEP-type porphyrins. When this type of porphyrins predominates, the oils are characterized by low maturity [12,13]. Such oils are formed in carbonaceous source beds with low clay content

and high sulfur content in organic substance. In addition, the oils with low maturity are characterized by the increased vanadium and nickel contents [8]. It was shown in [14,15] that the vanadium-to-nickel ratio (V/Ni) in heavy oils varies in broad range (4.7–14.8) and the vanadium content is largest in the specimens with the maximum content of these metals. Heavy oil with the increased vanadium content can be considered to be the source of natural porphyrins, which are accumulated in resin and asphaltene components [16]. An interest in petroleum porphyrins is also caused by their unique photophysical and catalytic properties. Porphyrins from oil stock could be used in the future as an alternative to synthetic porphyrins in such fields as catalysis [17–20], energetics [21], and medicine [11,22,23].

Employment of such analytical techniques as UV-Visible spectroscopy and mass spectrometry could identify and evaluate the abundance of petroleum vanadyl porphyrins [8,24]. However, interpretation accuracy of the recorded spectra is complicated due to the multi-component mixture of resin and asphaltene components, in which metalloporphyrins are accumulated. Consequently, preliminary isolation or concentration of metalloporphyrins along with purification from non-porphyrin components is necessary for their more accurate analysis. However, enrichment of high-purity vanadyl porphyrins from heavy residue is a labor-consuming and multiple-step procedure consisting of several stages, such as preliminary separation of asphaltenes and resins with subsequent multiple-stage chromatographic recovery of porphyrin concentrates on conventional sorbents (silica gel, alumina gel) in gradient elution mode [25]. In this case, chromatographic purification is the most labor-consuming stage, which also requires high consumption of adsorbent and organic solvents. This significantly restricts the potential of recovery of petroleum vanadyl porphyrins for the solution of various applied problems.

It has been shown in our previous works [26–29] that column chromatography using sulfocationite is a simpler and more effective method for purification of vanadyl porphyrin concentrate from asphaltenes or resins. Sulfocationite can be represented by silica gel modified with sulfuric acid, as well as sulfonated asphaltenes [30]. This approach, in contrast to conventional adsorbents, provides spectroscopically pure vanadyl porphyrins after one stage of chromatographic purification providing a minimum consumption of eluent and adsorbent. Investigation of the features of composition of vanadyl porphyrins in oil resins is of particular interest, because main fraction of vanadyl metal complexes remains in these fractions after separation of asphaltenes upon solvent deasphaltization. Therefore, investigation was carried out to reveal differences in the composition of vanadyl porphyrins recovered from the resins of heavy oils possessing high and low vanadium contents on the example of two deposits located in different oil-and-gas bearing basins.

## 2. Materials and Methods

All solvents and reagents used in this study were obtained from Sigma-Aldrich and used as received. As an adsorbent ASCG—silica gel (Activated Silica gel Coarse-grained Granulated) (GOST 3956-76) was used which was dried for 8 h at 150 °C.

To isolate asphaltenes from 10 g dehydrated oil, 40-fold volume excess of n-hexane was diluted and thoroughly mixed. After 24 h the obtained asphaltene precipitate was filtered and washed with boiling n-hexane up to decolorization of flowing solvent. The obtained asphaltenes washed from adsorbed maltenes, were eluted with benzene in a Soxhlet apparatus. Then, solvent was distilled from the resulting benzene solution of asphaltenes and asphaltenes dried at constant weight in a vacuum drying cabinet at a temperature of 80 °C.

After washing the asphaltenes, the maltene filtrate was attached to the basic maltene solution obtained by filtering the asphaltenes. Part of the n-hexane was removed so that the product is diluted with a solvent corresponding approximately to the ratio 1:3. The separation of maltenes on hydrocarbons (saturates) and resins (aromatics and heterorganic compounds) was done with the help of column chromatography using ASCG silica gel as the stationary phase. Silica gel was placed in a column with a diameter 1 cm and volume 50 mL using a sampling valve based on silica gel suspensions. Silica gel was impregnated

with n-hexane taken in quantity of 1g of a sample of 40 g of silica gel. After that, the maltene suspension was poured and maintained 2 h for maltene adsorption on silica gel. The rate of the product entry into the sorbent should not exceed 100–120 mL/h. For oil desorption, n-hexane was poured into the column through a dividing funnel. At the same time, the eluent was taken at a rate of 175–200 mL/h from the bottom of the column. Finally, the resins were eluted with an alcohol-benzene mixture. All samples of oils and resins after solvent distillation were dried in a vacuum at 80 °C up to a constant mass [31].

DMF extract from resins was obtained by adding an extraction agent to the resin suspension in the resin ratio extraction agent = 1:10 and boiling for 1 h. During the extraction of resins, a precipitate is formed. After cooling, the resulting mixture through a paper filter was filtered. The obtained DMF extract after distillation of solvent was brought to a constant mass in a drying cabinet at 60 °C.

The primary concentrate (PC) of vanadyl porphyrins from the DMF resin extract by column chromatography was obtained [26]. The DMF suspension of the extract was dissolved in a minimal amount of benzene and placed in a column (60 × 1 cm) filled with silica gel and eluted by solvents with increasing polarity. First, elution was carried out with benzene at the rate 6–9 of drops per second until there was a significant loss of color of the outgoing solution to remove fractions that do not contain nickel and vanadyl porphyrins (yellow and yellow–green) and those containing nickel porphyrins (orange). Next, elution with a mixture of benzene:trichloromethane in various ratios—80:20, 60:40, 40:60, 20:80 was carried out, after which the elution was carried out with pure trichloromethane. Finally, fractions containing vanadyl porphyrins were combined, and the solvent was distilled under a vacuum [27,28].

PC's chromatographic purification on sulfocationite with the necessary sulfuric acid content to extract purified vanadyl porphyrins (pVp) was carried out. First, a glass column with an inner diameter 12 mm (20 cm$^3$) was filled with a sorbent (silica gel impregnated with an 25% aqueous solution of sulfuric acid). Second, after impregnation by chloroform, 11.6 mg PCs were added with further chloroform elution. The eluent volume was 100 mL, and the elution rate was ~2 mL/min. Finally, the vanadyl porphyrin residues were washed out of the column with an 10% solution of isopropanol in chloroform. For spectrophotometry of the obtained fractions, the solvent was distilled to a constant mass, after which they were dissolved again in equal volumes of chloroform. Three experiments to obtain concentrates were carried out. The uncertainty was no more than 5%.

The electron absorption spectra in the UV and visible ranges were taken with a spectrophotometer "Spectrophotometer PE 5400 UV" in the range from 400 to 650 nm.in quartz cuvettes with a capacity of 5 mL and a solution layer thickness of 1 cm. A baseline approximating the background curve was drawn to account for the absorption of the non-porphyrin structure components. The intensity of the absorption band at 575 nm was calculated as the difference between the absorption maximum and the background curve. The vanadyl porphyrin content (C VP) in DMF resin extracts was determined spectrophotometrically by the formula [32]:

$$C\ VP\ (mg/100\ g) = 0.187\ h\ V/(m\ l)$$

where 0.187 is the conversion factor characterizing the absorption of the medium;

h—is the height of the maximum of the $\alpha$-absorption band at 575 ± 5 nm;
m—is the weight of the extract, g;
V—is the volume of the solution, mL;
l—cuvette thickness, cm

The vanadium content in all samples was determined by atomic absorption spectroscopy on an electrothermal atomization spectrometer «MGA-100» (Lumex, Russia). The liquid sample was dosed into the graphite cuvette of the spectrometer using variable volume microdispensers. The vanadium content was calculated from the calibration

curve obtained on the hydrocarbon matrix produced by Alfa Aesar, Specpure Vanadium (5000 µg/g) using a reference standard (Oil-based standard solution (Specpure®))

The infrared spectra of all samples were recorded on the device Spectrum One FTIR Spectrometer (Perkin Elmer, Norwalk, Connecticut, USA) in the range of 4000–400 $cm^{-1}$. The samples applied a toluene solution to a disk made of KBr and were dried to form a thin film. The spectra were processed and analyzed using the OPUS Version 6.5 software. The baseline and data normalization was used automatically. Based on the intensity of the characteristic absorption bands in the IR-Fourier spectra, spectral coefficients characterizing the structural and group composition of the studied objects were calculated [15,33]. Aliphaticity reflects the proportion of methylene and methyl groups relative to the proportion of aromatic C=C bonds and is calculated as the ratio of the total intensity of absorption bands due to methyl (1375 $cm^{-1}$) and methylene groups (720 $cm^{-1}$) to the intensity of the bands due to C=C bonds in aromatic moieties (1600 $cm^{-1}$). Aromaticity reflects the proportions of C=C bonds in aromatic moieties relative to the proportion of C–H bonds in aliphatic moieties and is calculated as the ratio of the intensity of the 1600$cm^{-1}$ band to the intensity of the absorption band at 1460 $cm^{-1}$. The ratio of intensities of methyl and methylene groups ($CH_3/CH_2$) was used for determination of branching of paraffin structures. Degree of condensation reflects the proportion of C=C bonds relative to that of C–H bonds in aromatic structures and is calculated as the ratio of the intensity of the 1600$cm^{-1}$ band to the total intensity of the absorption bands at 740 and 860 $cm^{-1}$. Degree of oxidation reflects the proportion of carbonyl groups R–C=O relative to C=C bonds in aromatic moieties and is calculated as the ratio of the intensity of the absorption band at 1700 $cm^{-1}$ to the intensity of the 1600 $cm^{-1}$ band. Sulfoxides reflects the proportion of the S=O bonds in the sulfoxide moieties relative to the proportion of C=C bonds in aromatic moieties and is calculated as the ratio of the intensity of the absorption band at 1030 $cm^{-1}$ to the intensity of the 1600 $cm^{-1}$ band. Sulfonates reflects the proportion of O = S = O bonds in sulfonate fragments relative (1160 $cm^{-1}$) to C = C bonds in aromatic fragments (1600 $cm^{-1}$).

The MALDI mass spectra purified vanadyl porphyrins recorded on a mass spectrometer UltraFlex III MALDI-TOF/TOF (Bruker Daltonik GmbH, Bremen, Germany) in a linear mode. The data were processed using software FlexAnalysis 3.0. The sample was ionized by nitrogen laser radiation with energy of 19 eV. Positively charged ions were recorded. The metal target MTP AnchorChipTM was used. Trihydroxyanthracene was used as a matrix. Molecular ions of vanadyl porphyrins of different homologs appear as peaks with mass 374+14n a.m.u. («n»—the number of methylene groups in the side substituents).

## 3. Results and Discussion

Vanadium content in HOs of Smorodinskoe deposit (HO no. 1) corresponds to 0.076 wt. % (Table 1), which is ca. six times as high as that in the HOs of Varadero deposit (HO no. 2). There are more asphaltenes and resins and there is a higher density in HO no. 2. The vanadium content in the resins of HO no. 2 is ca. 15 times as low as that in the resins of HO no. 1.

**Table 1.** Characteristics of heavy oils (HOs) and the resins isolated from them.

| HO | Density, at 20 °C, g/cm$^3$ | Content, wt. % | | | | |
|---|---|---|---|---|---|---|
| | | Asphaltenes | Resins | Hydrocarbons | Vanadium | |
| | | | | | in Oil | in Resins |
| no.1 | 0.9370 | 12.1 | 25.2 | 62.7 | 0.076 | 0.365 |
| no.2 | 1.0241 | 30.6 | 27.5 | 41.9 | 0.012 | 0.025 |

Comparison of Fourier IR spectra of the resins (Figure 1) and calculated spectral coefficients (Table 2) revealed particular differences of their structural-group composition.
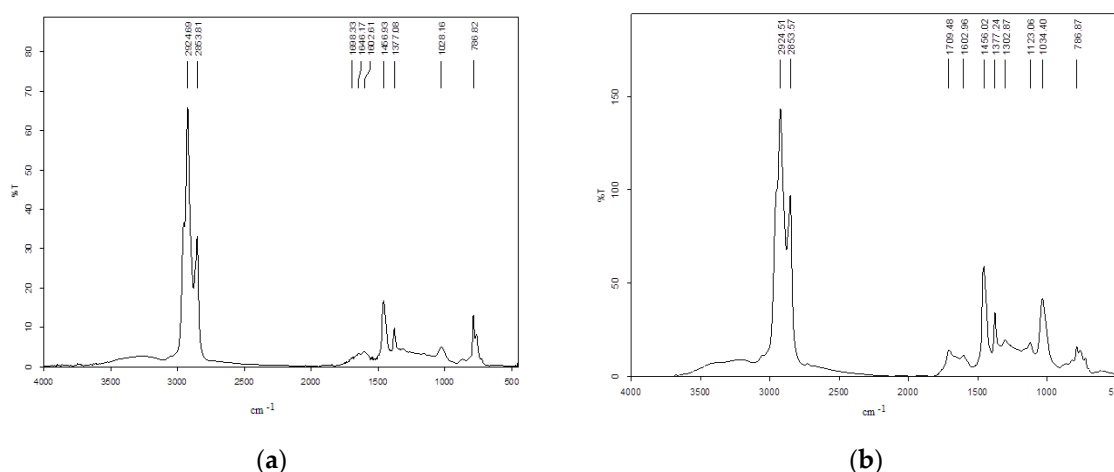
**Figure 1.** Fourier IR spectra of the resins of HO no. 1 (**a**) and HO no. 2 (**b**).

**Table 2.** Spectral coefficients of the resins.

| Resins of HO | Aliphaticity | Aromaticity | Branching | Condensation | Oxidation | Sulfoxides | Sulfonates |
|---|---|---|---|---|---|---|---|
| no.1 | 3.06 | 0.28 | 5.06 | 0.91 | 0.90 | 0.47 | 0.28 |
| no.2 | 3.48 | 0.26 | 3.48 | 0.72 | 1.22 | 3.62 | 1.29 |

Comparison of spectral coefficients derived from Fourier IR spectra of the resins of the HOs under study shows that HO nos. 1 and 2 differ marginally by the coefficient that characterizes aromaticity. There is a slight difference in spectral coefficients, which characterize the degree of condensation and aliphaticity, in the resins. Most distinct differences are observed upon comparison of the relative abundance of carboxylic and sulfo-groups to C=C bonds in aromatic fragments. Differences are also observed upon comparison of the relative abundance of C-H bonds in methyl fragments to C-H bonds in methylene groups. The resins of HO no. 2 are characterized by a higher content of oxygen-containing structures.

DMF extraction from the resins showed that the yields of the extracts differ marginally between HO nos. 1 and 2. In this case, vanadium and vanadyl porphyrin contents in DMF extracts from the resins of HO no. 1 are much higher (Table 3).

**Table 3.** Characteristics of DMF extract of the resins.

| Resins of HO | Yield of DMF Extract, wt. % | V content in Extracts, wt. % | VP Content, mg/100 g |
|---|---|---|---|
| no.1 | 42.5 | 0.430 | 796.7 |
| no.2 | 41.7 | 0.022 | 55.2 |

In the electronic absorption spectra of DMF extracts, a band in the near-UV region and called Soret band in name of its discoverer is the most intensive. In vanadyl porphyrins, the Soret band generally appears in the region of ~410 nm. In the visible spectral region, metalloporphyrin complexes have two absorption bands denoted as $\alpha$ and $\beta$. In vanadyl porphyrins, the $\alpha$ and $\beta$ absorption bands are in regions of ~570 and ~530 nm, respectively. The intensity of the absorption bands for the DMF extracts of HO no. 2 is lower than for the DMF extracts of HO no. 1. The absorbance band intensity ratio $K = \alpha/\beta$ in the spectra (Figure 2) at 570 nm ($\alpha$–band) and 530 nm ($\beta$-band) allows one to determine the dominant type of VPs in the obtained DMF extracts.
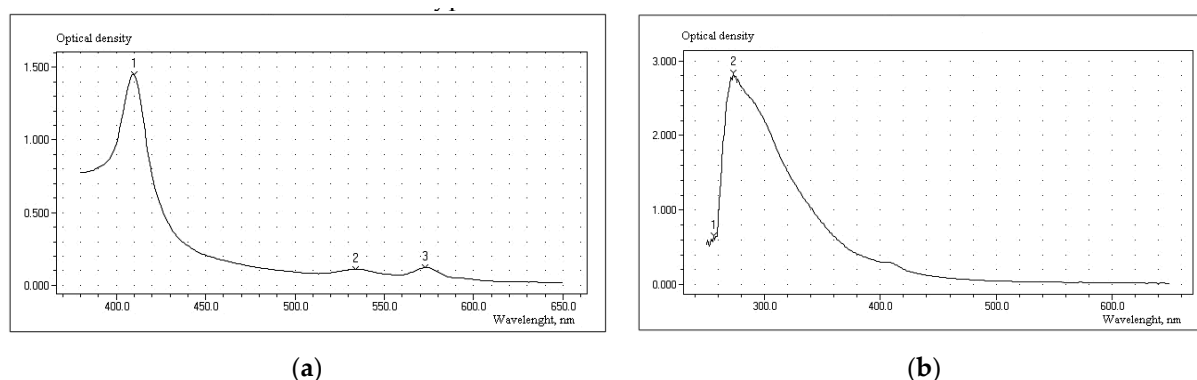
Figure 2. Absorption spectra of DMF extracts of the resins of HO nos. 1 (**a**) and 2 (**b**).

It is known [34–36] that DPEP predominate up to the values of 1.3; mixed-type porphyrins are dominant in the range of 1.3–2.00, more specifically, DPEP and etioporphyrins; and etioporphyrins predominate at the values higher than 2.0. As a result, it was determined that K = 1.9 for the DMF extract of the resins of HO no. 1 and K = 1.4 for the DMF extract of the resins of HO no. 2. Thus, it was determined that there is a mixture of DPEP- and etio-type porphyrins in the extracts at DMF extraction stage of the objects under study.

Comparison of Fourier IR spectra (Figure 3) and calculated spectral coefficients (Table 4) established that DMF extracts from the resins of HO nos. 1 and 2 differ significantly according to structural-group composition. There are higher aliphaticity and degree of branching, as well as high fraction of sulfo-groups and low degree of branching in structural-group composition of DMF extracts from the resins of HO no. 2. Condensation degree, aromaticity, and the content of carbonyl groups are higher in DMF extracts from the resins of HO no. 1.
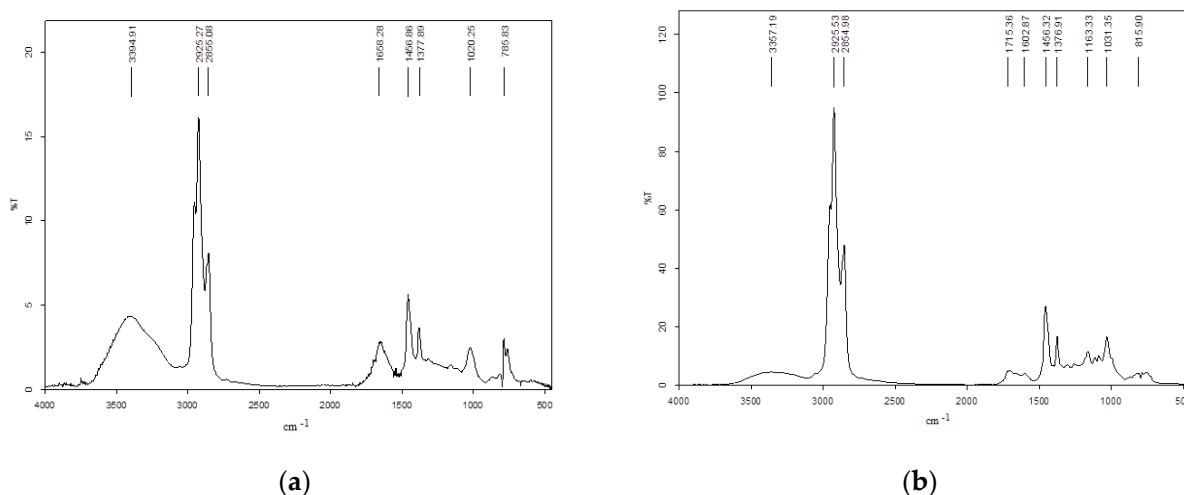


Figure 3. Fourier IR spectra of DMF extracts of the resins of HO nos. 1 (**a**) and 2 (**b**).

Table 4. Spectral coefficients of DMF extracts from resins.

| Resins of HO | Aliphaticity | Aromaticity | Branching | Condensation | Oxidation | Sulfoxides | Sulfonates |
|---|---|---|---|---|---|---|---|
| no.1 | 2.42 | 0.35 | 3.67 | 0.98 | 1.42 | 0.67 | 0.40 |
| no.2 | 5.01 | 0.15 | 5.39 | 0.66 | 0.90 | 1.24 | 0.60 |

As a result of stepwise chromatographic purification from DMF extracts of the resins, primary concentrate (PC) on silica gel and then, pVP on sulfocationite were isolated. It was shown that the yield of PC in the resins of HO no. 1 is less by a factor of ca. 1.6 than that in

the HO no. 2 (Table 5). The yield of pVP calculated on initial resins for HO no. 1 is higher by a factor of 11.1 than that of HO no. 2.

**Table 5.** Yield of PC and pVP from the resins of the oils.

| Resins of HO | Yield, wt. % | | | |
|---|---|---|---|---|
| | PC | | pVP | |
| | On Resins | On DMF Extract | On Resins | On PC |
| no.1 | 6.29 | 14.80 | 1.89 | 30.00 |
| no.2 | 3.92 | 9.40 | 0.17 | 4.50 |

UV-Visible absorption spectra (Figure 4) of pVP from the resins of HO nos. 1 and 2 recorded after stepwise chromatographic purification indicate an increase in the purity due to the decrease in the background absorption of non-porphyrin impurities. This statement is indirectly confirmed by the vanadium content in the PC and pVP isolated after chromatographic purification (Table 6) and the maximum concentration of oil vanadyl porphyrins is achieved in the latter case assuming their mean molecular mass.
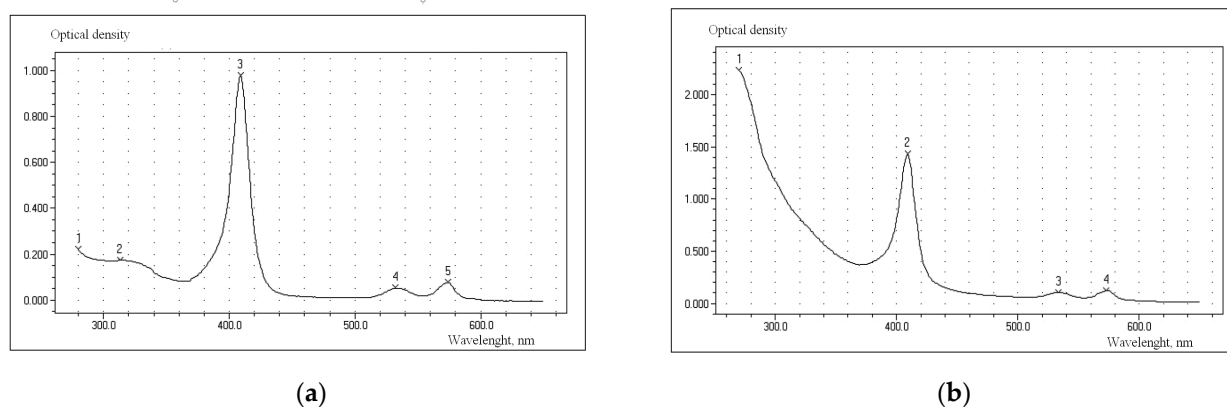


(**a**)                                    (**b**)

**Figure 4.** Electronic absorption spectra of pVP from the resins of HO nos. 1 (**a**) and 2 (**b**).

**Table 6.** Vanadium content in PC and pVP from resins.

| Resins of HO | Content of V, wt. % | |
|---|---|---|
| | PC | pVP |
| no.1 | 2.71 | 7.13 |
| no.2 | 0.19 | 3.24 |

The achieved degree of purification of VPs allowed to record MALDI-TOF mass spectra of the concentrates of vanadyl porphyrins (VPs) from DMF extracts of the resins of HO nos. 1 and 2 at m/z 300–1500. Comparison of MALDI mass spectra in the range of m/z 460–640 revealed principal features of the composition of vanadyl porphyrins in the concentrates. In the recorded mass spectra of the fractions (Figures 5 and 6), the peaks of $C_{27}$-$C_{39}$ homologs for HO no. 1 and $C_{28}$-$C_{39}$ homologs for HO no. 2 were identified, which correspond to the most common types of oil vanadyl porphyrins: etioporphyrin and deoxophylloerythroetioporphyrin (DPEP). Vanadyl porphyrins with higher mass were not analyzed due to noises in spectra at m/z > 650. Noticeable complication of the spectrum at higher masses is caused by the presence of impurities and lack of resolution.
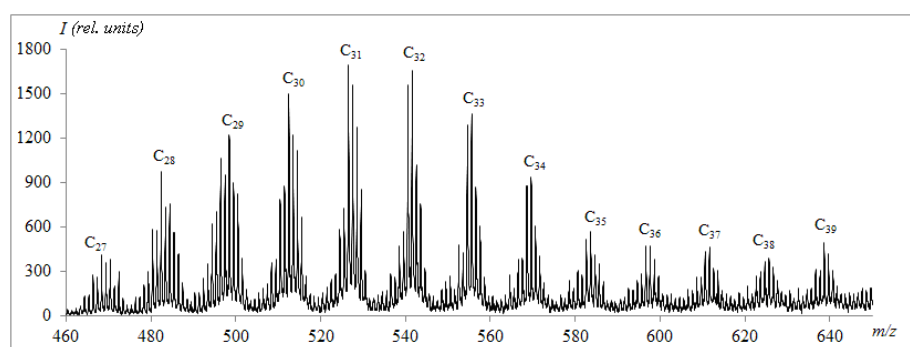
**Figure 5.** MALDI-TOF mass spectrum of pVP from DMF extract of the resins of HO no. 1.
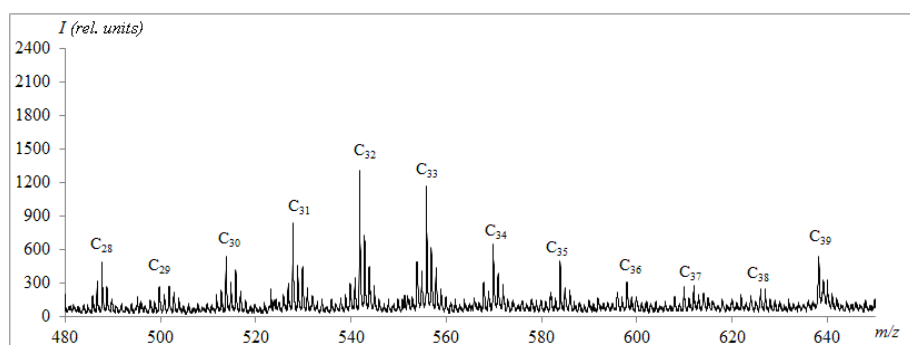


**Figure 6.** MALDI-TOF mass spectrum of pVP from DMF extract of the resins of HO no. 2.

In the case of vanadyl porphyrins of HO no. 1, the maximum content of etio type is in $C_{31}$ homolog (m/z = 529.22 [M]+·), whereas that of DPEP type is in $C_{32}$ homolog (m/z = 541.22 [M]+·). The content of etio-type vanadyl porphyrins is inferior to DPEP-type porphyrins $\sum$DPEP/$\sum$ETIO = 2.93), which is the criterion of the maturation stage of oil. In the case of pVP from the resins of HO no. 2, the maximum content of etio-type corresponds to the $C_{30}$ homolog (m/z = 515.20 [M]+·), while that of DPEP type corresponds to $C_{32}$ homolog (m/z = 541.22 [M]+·). The content of etio-type vanadyl porphyrins is also less than that of DPEP-type porphyrins ($\sum$DPEP/$\sum$ETIO = 3.77).

To obtain detailed information from the MALDI-TOF mass spectra, abundance of other most common types of VPs in the fractions was studied. Because metalloporphyrins are known to form molecular ions [M]+· during ionization using MALDI and laser desorption/ionization (LDI), the VPs were semi-quantified from relative intensities of corresponding ions [M]+·. Six following types of VPs were analyzed: etio type (m/z 473+14n); DPEP type (m/z 471+14n); dicyclic DPEP type (Di-DPEP) (m/z 469+14n), rhodo-etioporphyrins (Rhodo-Etio) (m/z 467+14n), Rhodo-DPEP type (m/z 465+14n), and Rhodo-Di-DPEP) (m/z 463+14n), where n is the integer from 0 to 14. Their [M]+· signals were obtained from the spectra and used for plotting histograms describing the numeric distribution of various types of VPs in the fraction (Figure 7). According to Figure 7, DPEP type is the most abundant type of vanadyl porphyrins discovered for the VP concentrate from DMF extract of the resins of HO nos. 1 and 2.
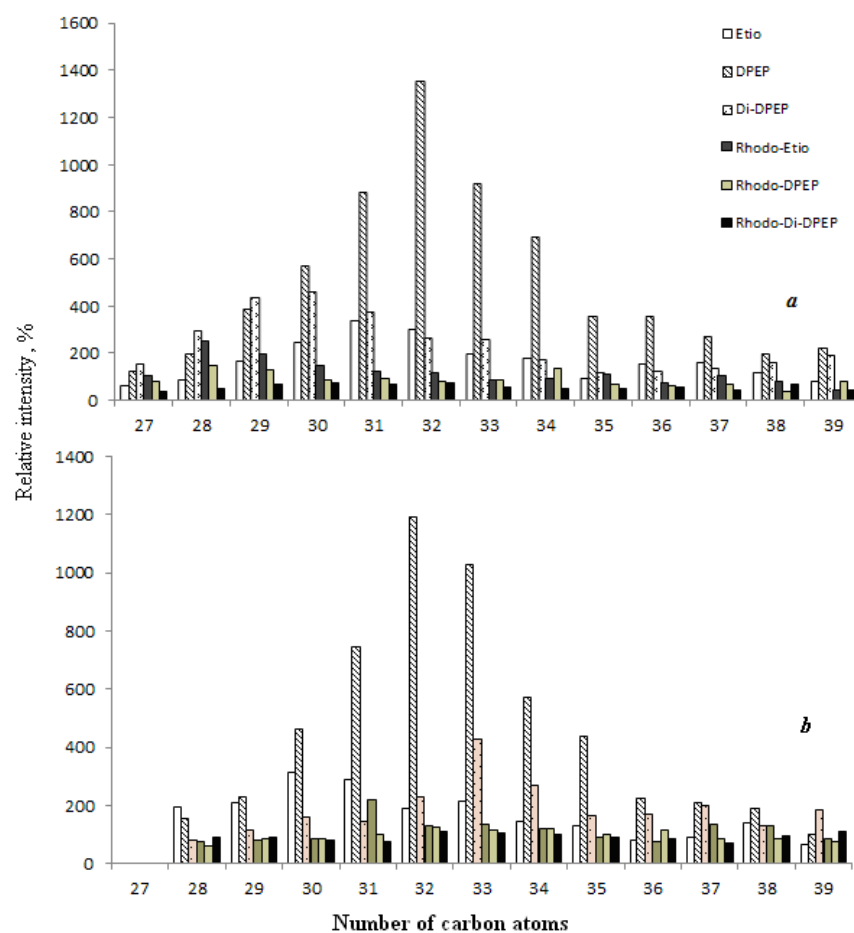
**Figure 7.** Distribution of various types of vanadyl porphyrins in pVP from DMF extract from the resins of HO nos. 1 (**a**) and 2 (**b**) according to the data of MALDI-TOF mass spectra.

The diagram (Figures 8 and 9) shows the relative abundance (in %) of various types of VPs in pVP from the resins of HO nos. 1 and 2.
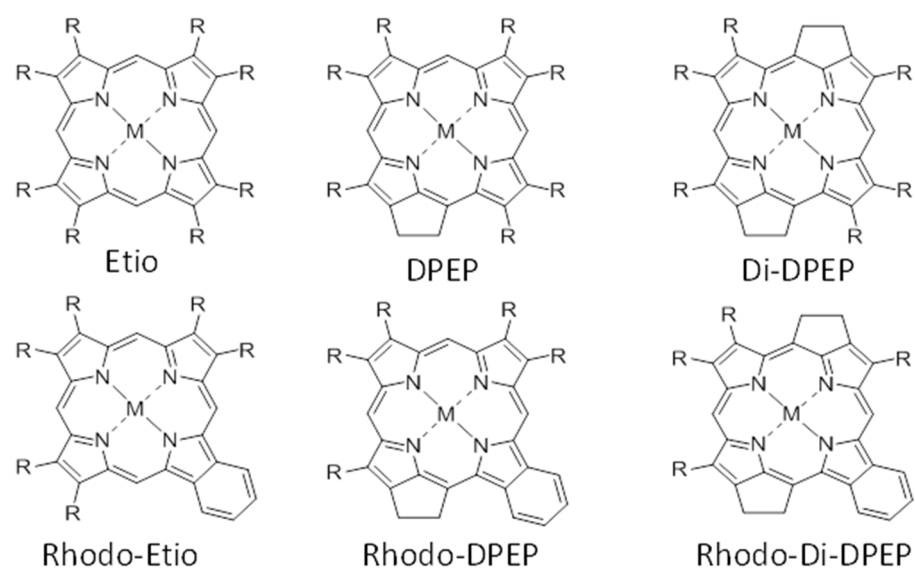


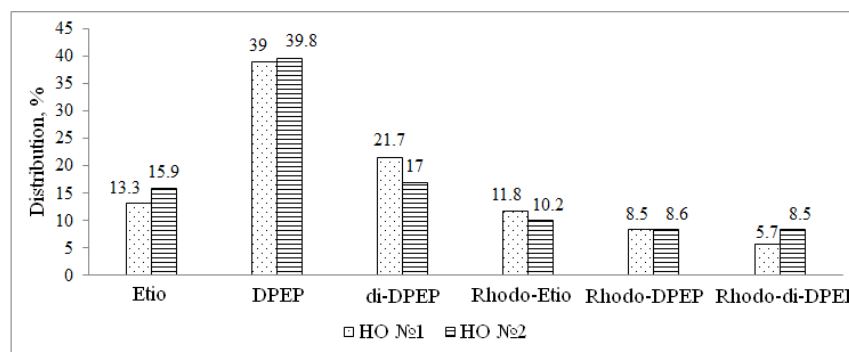**Figure 8.** Representatives of the most common types of petroleum porphyrins.

**Figure 9.** Relative abundance of various types of vanadyl porphyrins in pVP from the resins of HO nos. 1 and 2.

In HO no. 2, the content of Rhodo-Di-DPEP-type VPs is higher by a factor of 1.5 than that of HO no. 1. The content of Di-DPEP- and Rhodo-ETIO-type vanadyl porphyrins in HO no. 1 is higher than that in HO no. 2 by factors of 1.3 and 1.2, respectively. Thus, different ranges of vanadyl porphyrin homologs were identified in the isolated concentrates from the resins for HO nos. 1 and 2. In HO no. 1, the peaks of $C_{27}$-$C_{39}$ homologs were identified, with the maximum for $C_{32}$ homolog. In HO no. 2, the peaks of $C_{28}$-$C_{39}$ homologs were identified, with the maximum for $C_{30}$ homolog (Figure 10). Even though the highest content corresponds to the vanadyl porphyrins of deoxophylloerythroetioporphyrin (DPEP type), there are differences of the abundance values of most common types of vanadyl porphyrins in the oils under study, such as etio-, DPEP-, Di-DPEP, Rhodo-Etio, Rhodo-DPEP, and Rhodo-Di-DPEP. The content of Rhodo-DPEP- and Rhodo-Di-DPEP-type VPs in the resins of HO no. 2 is higher than that of HO no. 1 by a factors of 1.3 and 3.5, respectively, along with a decrease in the content of other types of VPs by a factor of 1.1–1.6.
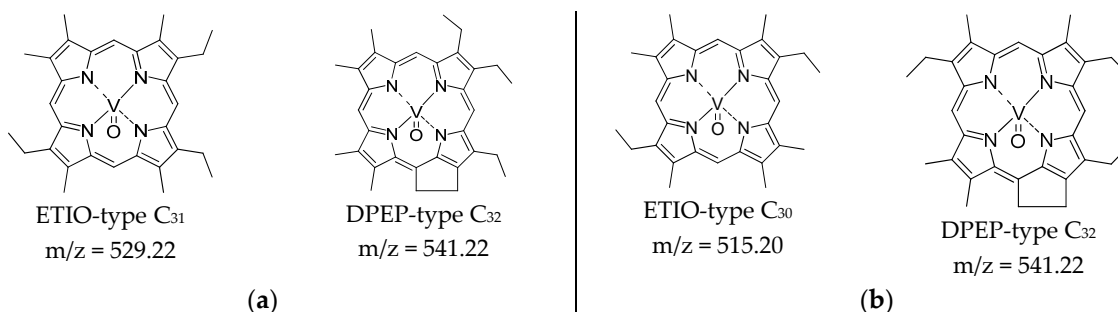


| ETIO-type $C_{31}$ | DPEP-type $C_{32}$ | ETIO-type $C_{30}$ | DPEP-type $C_{32}$ |
| :---: | :---: | :---: | :---: |
| m/z = 529.22 | m/z = 541.22 | m/z = 515.20 | m/z = 541.22 |
| (**a**) | | (**b**) | |

**Figure 10.** Possible structures of dominant homologs of vanadyl porphyrins of etio and DPEP types in pVP from the resins of HO nos. 1 (**a**) and 2 (**b**).

## 4. Conclusions

This study has revealed features of the composition of vanadyl porphyrins isolated from the resins of heavy oil of Smorodinskoe deposit (Russia) with high vanadium content and Varadero deposit (Cuba) with low vanadium content. The vanadium content in the resins of oil of Smorodinskoe deposit is ca. 15 times as high as that of Varadero deposit. Comparison of the spectral coefficients of Fourier IR spectra has shown differences in the structural-group composition of the resins. The resins with low vanadium content are characterized by a higher condensation degree and higher fraction of carbonyl and sulfo-groups in the molecules. Aliphaticity and aromaticity of the resins of the oils under study differ marginally.

To recover and purify vanadyl porphyrins from the resins, extraction by *N,N*–dimethylformamide (DMF) with subsequent two-stage column chromatography on silica gel and sulfocationite were employed. It was shown that the yield of purified vanadyl porphyrins from the resins with high vanadium content is much higher and corre-

sponds to 1.89 wt. %. As a result of analysis of MALDI mass spectra in the range of m/z 460–640, the peaks of $C_{27}$-$C_{39}$ homologs for the resins with the high vanadium content and $C_{28}$-$C_{39}$ homologs for the resins with the low vanadium content were identified in the specimens of purified vanadyl porphyrins. Analysis of distribution of the most common types of VPs has shown that the maximum abundance of etio-type vanadyl porphyrins in the resins with high vanadium content is in the $C_{31}$ homolog (m/z = 529.22 [M]+·), whereas DPEP type is mainly represented by $C_{32}$ homolog (m/z = 541.22 [M]+·); in this case, DPEP type is dominant ($\sum$DPEP/$\sum$ETIO = 2.93). In the resins with low vanadium content, the maximum abundance of etio-type vanadyl porphyrins is in the $C_{30}$ homolog (m/z = 515.20 [M]+·), while that of DPEP type is in the $C_{32}$ homolog (m/z = 541.22 [M]+·); in this, case, DPEP type is dominant ($\sum$DPEP/$\sum$ETIO = 3.77).

## References

1. Speight, J.G. *Heavy Oil Recovery and Upgrading*, 1st ed.; Gulf Professional Publishing: Houston, TX, USA, 2019; 81p.
2. Meyer, R.F.; Attanasi, E.D.; Freeman, P.A. *Heavy Oil and Natural Bitumen Resources in Geological Basins of the World*; U.S. Geological Survey Open-File Report: Reston, VA, USA, 2007; 1084p.
3. Ancheyta, J. *Modeling of Processes and Reactors for Upgrading of Heavy Petroleum*, 1st ed.; CRC Press, Taylor & Francis Group: Boca Raton, FL, USA, 2013; 524p.
4. Okunev, A.G.; Parkhomchuk, E.V.; Lysikov, A.I.; Parunin, P.D.; Semeykina, V.S.; Parmon, V.N. Catalytic hydroprocessing of heavy oil feedstocks. *Russ. Chem. Rev.* **2015**, *84*, 981–999. [CrossRef]
5. Jones, D.S.J. An introduction to crude oil and its processing. In *Handbook of Petroleum Processing*; James, L.C., Mansoori, G.A., Eds.; Springer: Dordrecht, The Netherlands, 2008; pp. 1–46.
6. Khadzhiev, S.N.; Kadiev, K.M.; Kadieva, M.K. Synthesis and properties of nanosized systems as efficient catalysts for hydroconversion of heavy petroleum feedstock. *Pet. Chem.* **2014**, *54*, 323–346. [CrossRef]
7. Dechaine, G.; Gray, M. Chemistry and association of vanadium compounds in heavy oil and bitumen, and implications for their selective removal. *Energy Fuels* **2010**, *24*, 2795–2808. [CrossRef]
8. Zhao, X.; Chunming, X.; Shi, Q. Porphyrins in heavy petroleums: A review. In *Structure and Modeling of Complex Petroleum Mixtures*; Chunming, X., Shi, Q., Eds.; Springer International Publishing: Cham, Switzerland, 2016; pp. 39–70.
9. Serebrennikova, O.V.; Filippova, T.Y.; Krasnoyarova, N.A. Interrelation between the composition of alkanes and metalloporphyrins in crude oils and rock organic matter as a reflection of formation conditions of oil-bearing strata in the southeast of West Siberia. *Pet. Chem.* **2003**, *43*, 145–149.
10. Izmailova, D.Z.; Serebrennikov, V.M.; Mozzhelina, T.K.; Serebrennikova, O.V. Features of the molecular composition of metalloporphyrins of crude oils of the Volga-Urals oil- and gas-bearing province. *Pet. Chem.* **1996**, *36*, 111–117.
11. Huang, H.; Song, W.; Rieffel, J.; Lovell, J.F. Emerging applications of porphyrins in photomedicine. *Front. Phys.* **2015**, *3*, 23. [CrossRef]
12. Zheng, F.; Zhu, G.; Chen, Z.; Zhao, Q.; Shi, Q. Molecular composition of vanadyl porphyrins in the gilsonite. *J. Fuel Chem. Technol.* **2020**, *48*, 562–567. [CrossRef]
13. Isaji, Y.; Kawahata, H.; Takano, Y.; Ogawa, N.O.; Kuroda, J.; Yoshimura, T.; Lugli, S.; Manzi, V.; Roveri, M.; Diazotrophy, N.O. Drives primary production in the Organic-Rich shales deposited under a stratified environment during the Messinian salinity crisis. *Front. Earth Sci.* **2019**, *7*, 85. [CrossRef]
14. Yakubov, M.R.; Milordov, D.V.; Yakubova, S.G.; Borisov, D.N.; Ivanov, V.T.; Sinyashin, K.O. Concentrations of vanadium and nickel and their ratio in heavy oil asphaltenes. *Pet. Chem.* **2016**, *56*, 16–20. [CrossRef]

15. Yakubov, M.R.; Sinyashin, K.O.; Abilova, G.R.; Tazeeva, E.G.; Milordov, D.V.; Yakubova, S.G.; Borisov, D.N.; Gryaznov, P.I.; Mironov, N.A.; Borisova, Y.Y. Differentiation of heavy oils according to the vanadium and nickel content in asphaltenes and resins. *Pet. Chem.* **2017**, *56*, 849–854. [CrossRef]
16. Mello, A.P.; Pereira, J.S.F.; Moraes, D.P.; Dressler, V.L.; Flores, E.M.M.; Knapp, G. Nickel, vanadium and sulfur determination by inductively coupled plasma optical emission spectrometry in crude oil distillation residues after microwave-induced combustion. *J. Anal. At. Spectrom.* **2009**, *24*, 911–916. [CrossRef]
17. Barona-Castano, J.C.; Carmona-Vargas, C.C.; Brocksom, T.J.; de Oliveira, K.T. Porphyrins as catalysts in scalable organic reactions. *Molecules* **2016**, *21*, 310. [CrossRef] [PubMed]
18. Che, C.-M.; Huang, J.-S. Metalloporphyrin-based oxidation systems: From biomimetic reactions to application in organic synthesis. *Chem. Commun* **2009**, *27*, 3996–4015. [CrossRef] [PubMed]
19. Nakagaki, S.; Ferreira, G.; Ucoski, G.; Dias de Freitas Castro, K. Chemical reactions catalyzed by metalloporphyrin-based metal-organic frameworks. *Molecules* **2013**, *18*, 7279–7308. [CrossRef] [PubMed]
20. Zhang, J.-L.; Che, C.-M. Soluble polymer-supported ruthenium porphyrin catalysts for epoxidation, cyclopropanation, and aziridination of alkenes. *Org. Lett.* **2002**, *4*, 1911–1914. [CrossRef]
21. Li, L.L.; Diau, E.W.G. Porphyrin-sensitized solar cells. *Chem. Soc. Rev.* **2013**, *42*, 291–304. [CrossRef]
22. Caron, S.; Dugger, R.W.; Ruggeri, S.G.; Ragan, J.A.; Brown Ripin, D.H. Large-scale oxidations in the pharmaceutical industry. *Chem. Rev.* **2006**, *106*, 2943–2989. [CrossRef] [PubMed]
23. Srour, H.; Jalkh, J.; le Maux, P.; Chevance, S.; Kobeissi, M.; Simonneaux, G. Asymmetric oxidation of sulfides by hydrogen peroxide catalyzed by chiral manganese porphyrins in water/methanol solution. *J. Mol. Catal. A Chem.* **2013**, *370*, 75–79. [CrossRef]
24. Mironov, N.A.; Milordov, D.V.; Abilova, G.R.; Yakubova, S.G.; Yakubov, M.R. Methods for studying petroleum porphyrins (Review). *Pet. Chem.* **2019**, *59*, 1077–1091. [CrossRef]
25. Rytting, B.M.; Singh, I.D.; Kilpatrick, P.K.; Harper, M.R.; Mennito, A.S.; Zhang, Y. Ultrahigh-purity vanadyl petroporphyrins. *Energy Fuels* **2018**, *32*, 5711–5724. [CrossRef]
26. Milordov, D.V.; Mironov, N.A.; Abilova, G.R.; Tazeeva, E.G.; Yakubova, S.G.; Yakubov, M.R. Obtaining pure vanadyl porphyrins from heavy petroleum residue to create catalysts for various processes. *Katal. V Promyshlennosti* **2020**, *20*, 352–358. [CrossRef]
27. Mironov, N.A.; Sinyashin, K.O.; Abilova, G.R.; Tazeeva, E.G.; Milordov, D.V.; Yakubova, S.G.; Borisov, D.N.; Gryaznov, P.I.; Borisova, Y.Y.; Yakubov, M.R. Chromatographic isolation of vanadyl porphyrins from heavy oil resins. *Russ. Chem. Bull. Int. Ed.* **2017**, *66*, 1450–1455. [CrossRef]
28. Mironov, N.A.; Abilova, G.R.; Sinyashin, K.O.; Gryaznov, P.I.; Borisova, Y.Y.; Milordov, D.V.; Tazeeva, E.G.; Yakubova, S.G.; Borisov, D.N.; Yakubov, M.R. Chromatographic isolation of petroleum vanadyl porphyrins using sulfocationites as sorbents. *Energy Fuels* **2018**, *32*, 161–168. [CrossRef]
29. Mironov, N.A.; Milordov, D.V.; Tazeeva, E.G.; Abilova, G.R.; Tazeev, D.I.; Morozov, V.I.; Yakubova, S.G.; Yakubov, M.R. Influence of the composition of the sulfuric acid cation exchanger on the efficiency of chromatographic purification of petroleum vanadyl porphyrins. *Russ. J. Appl. Chem.* **2020**, *93*, 888–896. [CrossRef]
30. Yakubov, M.R.; Gryaznov, P.I.; Yakubova, S.G.; Tazeeva, E.G.; Mironov, N.A.; Milordov, D.V. Structural-group composition and properties of heavy oil asphaltenes modified with sulfuric acid. *Pet. Sci. Technol.* **2016**, *34*, 1805–1811. [CrossRef]
31. Demirbas, A.; Taylan, O. Removing of resins from crude oils. *Pet. Sci. Technol.* **2016**, *34*, 771–777. [CrossRef]
32. Yakubov, M.R.; Milordov, D.V.; Yakubova, S.G.; Borisov, D.N.; Gryaznov, P.I.; Mironov, N.A.; Abilova, G.R.; Borisova, Y.Y.; Tazeeva, E.G. Features of the composition of vanadyl porphyrins in the crude extract of asphaltenes of heavy oil with high vanadium content. *Pet. Sci. Technol.* **2016**, *34*, 177–183. [CrossRef]
33. Taheria, Z.; Dehaghani, A.S.; Ayatollahi, S.; Kharrat, R. A new insight to the assessment of asphaltene characterization by using fortier transformed infrared spectroscopy. *J. Petrol. Sci. Eng.* **2021**, *205*, 108824–108832. [CrossRef]
34. Dolphin, D. *The Porphyrins V1: Structure and Synthesis, Part A*, 1st ed.; Academic Press: New York, NY, USA, 1978; 664p.
35. Doukkali, A.; Saoiabi, A.; Zrineh, A.; Hamad, M.; Ferhat, M.; Barbe, J.M.; Guilard, R. Separation and identification of petroporphyrins extracted from the oil shales of Tarfaya. *Geochem. Study. Fuel* **2002**, *81*, 467–472. [CrossRef]
36. Gao, Y.-Y.; Shen, B.-X.; Liu, J.-C. The structure identification of vanadium porphyrins in Venezuela Crude Oil. *Energy Sources Part A Recovery Util. Environ. Eff.* **2012**, *34*, 2260–2267. [CrossRef]